

# the Key of Parameter Skew in Federated Learning

Sifan Wang\*, Junfeng Liao\*, Ye Yuan, Riquan Zhang†

School of Statistics and Information  
Shanghai University of International Business and Economics  
Shanghai, 201620 China  
{23349111, 23349089, yuany, rqzhang}@suibe.edu.cn

## Abstract

Federated Learning (FL) has emerged as an excellent solution for performing deep learning on different data owners without exchanging raw data. However, statistical heterogeneity in FL presents a key challenge, leading to a phenomenon of skewness in local model parameter distributions that researchers have largely overlooked. In this work, we propose the concept of *parameter skew* to describe the phenomenon that can substantially affect the accuracy of global model parameter estimation. Additionally, we introduce FedSA, an aggregation strategy to obtain a high-quality global model, to address the implication from *parameter skew*. Specifically, we categorize parameters into high-dispersion and low-dispersion groups based on the coefficient of variation. For high-dispersion parameters, Micro-Classes (MIC) and Macro-Classes (MAC) represent the dispersion at the micro and macro levels, respectively, forming the foundation of FedSA. To evaluate the effectiveness of FedSA, we conduct extensive experiments with different FL algorithms on three computer vision datasets. FedSA outperforms eight state-of-the-art baselines by about 4.7% in test accuracy.

## 1 Introduction

Federated Learning (FL) is a classical paradigm of distributed training that mitigates the communication barriers between datasets of different clients while enabling synchronous training with ensured data privacy (Shokri and Shmatikov 2015; Yang et al. 2019). With the increasing attention to data privacy issues in the industry, FL has been widely applied in fields such as medicine and the Internet (Yang et al. 2021; Wu et al. 2020; Liu et al. 2020). FL has become an important and widely researched area in the field of Machine Learning. FedAVG (McMahan et al. 2017), a fundamental algorithm in FL, aggregates trained local models that are transmitted to the server in each round to update the global model, while the raw data from clients is not exchanged. A key challenge in FL is the heterogeneity of data distribution on different parties (Chen et al. 2022; Shang et al. 2022; T Dinh, Tran, and Nguyen 2020). In the real world, data among parties can be non-Independent and Identically Distributed (non-IID), which makes dispersion among parameters of clients' models be enlarged, as shown

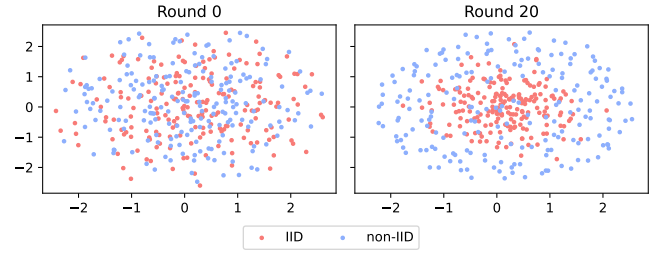


Figure 1: T-SNE visualizations illustrate the changes in the distribution of local model parameters during training under both IID and non-IID. Under IID, parameters gradually converge during training, whereas under non-IID, they remain scattered.

in Figure 1. Due to the dispersion, the global model may deviate from the optimal solution after aggregating local models from clients (Karimireddy et al. 2020).

Several traditional federated learning (tFL) and personalized federated learning (pFL) studies have been conducted to address the non-IID issue during the training phase of local models (Li et al. 2020; Wang et al. 2020a,b; Kairouz et al. 2021; Li et al. 2021; Oh, Kim, and Yun 2021; Zhang et al. 2023). For instance, FedProx (Li et al. 2020) constrains the updates of local models using the  $\ell_2$ -norm distance, while FAVOR (Wang et al. 2020a) selects a subset of clients in each training round. Furthermore, FedMA (Wang et al. 2020b) utilizes statistical methods to alleviate data heterogeneity. Ditto (Li et al. 2021) derives personalized models by incorporating regularization terms for each client to leverage information from the global model. FedBABU (Oh, Kim, and Yun 2021) fine-tunes the classifier of the global model to obtain personalized models for individual clients. FedALA (Zhang et al. 2023) proposes an adaptive aggregation strategy, enabling personalized models to selectively absorb information from the global model. However, these methods are unable to concentrate on the discrepancies among parameters of local models, while focusing on the architecture of the model instead.

Our method is based on an observation, namely *parameter skew* we proposed: as shown in Figure 1, t-SNE (Van der Maaten and Hinton 2008) is used to visualize the distribution of local model parameters, revealing that the non-IID

\*These authors contributed equally.

†Corresponding author.

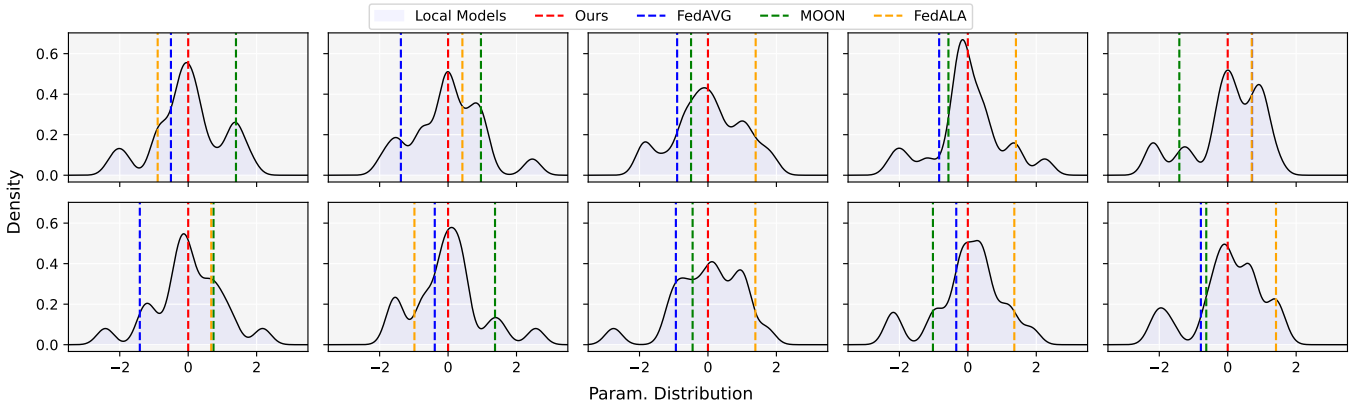


Figure 2: **The distribution of parameters of local models, FedSA(ours), MOON, FedALA, and FedAVG.** Figure 2 clearly illustrates the presence of *parameter skew*. Our method aligns closely with the main peak of the distribution, indicating that FedSA effectively captures the central tendency under *parameter skew*. In contrast, other methods fail to address this issue, resulting in a deviation from the main peak.

issue causes dispersion among parameters of models with the same structure trained on different clients. Owing to the varying label distributions of data across different clients, models with identical structures learn disparate information on different clients, which leads to considerable variations in certain parameter values among local models. However, according to the Law of Large Numbers (Hsu and Robbins 1947), skewness in the sample distribution can introduce significant bias into estimators, such as the mean, thereby reducing their accuracy. The process of deriving a global model from local models can be seen as a parameter estimation task, where *parameter skew* can significantly affect global model parameters. As illustrated in Figure 2, distribution of local models’ parameters shows obvious skewness. Furthermore, FedAVG averages local model parameters to estimate global model parameters, potentially causing them to deviate from the central tendency and thereby weakening the model’s generalization ability. To tackle the problem, we propose a novel FL algorithm, FedSA shown in Figure 3. We leverage the coefficient of variation (Brown 1998) to category parameters into high-dispersion and low-dispersion. We continue to use the FedAVG process for parameters with low dispersion, while for high-dispersion parameters, we describe the extent of dispersion from both micro and macro perspectives, resulting in Micro-Classes (MIC) and Macro-Classes (MAC). We assign weights to parameters according to the MIC and MAC distributions, accounting for varying degrees of dispersion, to construct the global model.

To evaluate the effectiveness of FedSA, we conducted a comparative analysis with eight FL algorithms on CIFAR-10/100 (Krizhevsky, Hinton et al. 2009) and Tiny-ImageNet (Chrabaszcz, Loshchilov, and Hutter 2017) datasets. The results, presented in Table 1, indicate that our method surpasses other state-of-the-art (SOTA) methods. Additionally, we visualized the distribution of each parameter to illustrate the rationale behind FedSA. In summary, our contributions are as follows:

- We propose the *parameter skew* resulting from hetero-

geneity and analyze its implications for the global model in FL.

- We introduce a novel FL algorithm, FedSA, which addresses the non-IID issue by leveraging *parameter skew* to obtain Micro-Classes (MIC) and Macro-Classes (MAC). Additionally, we analyze the rationale behind FedSA and elucidate the reasons why other FL methods fail to achieve optimal performance.
- We conducted comprehensive experiments comparing FedSA with other baseline methods using three widely used datasets. FedSA outperformed eight SOTA methods, achieving up to a 4.7% improvement in test accuracy while incurring lower computational costs.

## 2 Related Work

### Traditional Federated Learning

The traditional federated learning model, FedAVG (McMahan et al. 2017), derives a global model through the aggregation of local models. Nevertheless, the heterogeneity of data across different clients detrimentally affects the performance of FedAVG. To address this challenge, FedProx (Li et al. 2020) enhances the stability and generalization capability of the algorithm by incorporating a proximal term. FAVOR (Wang et al. 2020a) ameliorates the bias induced by non-IID data by selecting a subset of participating clients in each training round. FedMA (Wang et al. 2020b) introduces a layer-wise approach that leverages Bayesian non-parametric methods to mitigate data heterogeneity. FedGen (Venkateswaran et al. 2023) employs a masking function to address spurious correlations and biases in the training data, enabling clients to identify and differentiate between spurious and invariant features. MOON (Li, He, and Song 2021a) capitalizes on the similarity between models to refine the training process of individual clients, achieving superior performance in federated learning for image domains. FedNTD (Lee et al. 2022) utilizes Knowledge Distillation to alleviate

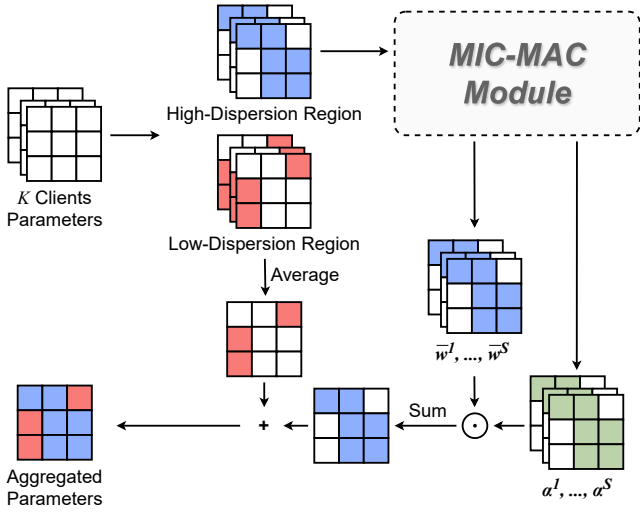


Figure 3: **The architecture of FedSA.** We take a 3x3 convolutional kernel as an example. The blue region represents the high-dispersion parameters, while the red region represents the low-dispersion parameters. The MIC-MAC Module is illustrated in Figure 4.

the issue of data heterogeneity, concentrating solely on data that has not been accurately predicted.

### Personalized Federated Learning

Recently, personalized federated learning (pFL) has attracted significant attention within the research community due to its superior performance in addressing data heterogeneity challenges (Kairouz et al. 2021). In the Ditto framework (Li et al. 2021), each client incorporates an optimal term to extract information from the global model, learning an additional personalized model. FedBABU (Oh, Kim, and Yun 2021) fine-tunes the classifier within the global model using client-specific data to develop personalized models for each client. FedALA (Zhang et al. 2023) introduces an adaptive aggregation strategy to selectively assimilate information from the global model.

## 3 Our Method

### Problem Statement

Federated Learning aims to train a global model on the server while ensuring the data privacy of clients. Suppose there are  $K$  clients, with the data of the  $i$ -th client denoted as  $D^i$ . Let  $\mathcal{L}(\cdot, \cdot)$  represent the loss function of each local model. Typically, we minimize the loss  $L$ , as defined in Equation (1), to obtain the global model  $f(\cdot)$ .

$$L = \frac{\sum_{i=1}^K |D^i| \cdot \mathbb{E}_{(X^i, Y^i) \sim D^i} [\mathcal{L}(f(X^i), Y^i)]}{\sum_{i=1}^K |D^i|}. \quad (1)$$

### Methodology

In our experiments, we observe that the non-IID issue exacerbates the dispersion among local models due to the varying

information available to different clients. Conversely, under the IID hypothesis, the dispersion is significantly reduced, shown in Figure 1. Motivated by the aforementioned observations, we propose FedSA, a novel and effective FL algorithm, shown in Figure 3. FedSA aims to enhance the global model update strategy by distributing the weight of each parameter according to the extent of *parameter skew*.

#### Algorithm 1: FedSA

**Input :**  $K$ : clients,  $\rho$ : client joining ratio,  $\mathcal{L}$ : loss function,  $\Theta^0$ : initial global model,  $\mathbf{C}$ : classes of MIC,  $\mathbf{S}$ : classes of MAC,  $cv_t$ : the threshold between high-dispersion and low-dispersion,  $sim_t$ : threshold of clients' similarity,  $T$ : round of training.

**Output:** High quality global model  $\hat{\Theta}^T$ .

- 1: **for** iteration  $t = 1, \dots, T$  **do**
- 2:   Server sends  $\Theta^t$  to clients to initialize local models.
- 3:   Training local models  $\hat{\Theta}_1^t, \dots, \hat{\Theta}_K^t$ .
- 4:   Local models parameters  $W = \{\hat{\Theta}_1^t, \dots, \hat{\Theta}_K^t\}$ .
- 5:   **for**  $j$  in  $W$  **do**
- 6:     Computing  $cv_j$  (2) (3) (4).
- 7:     Obtaining  $\mathbf{r}_j^l$  and  $\mathbf{r}_j^h$  (5) (6).
- 8:     Computing MIC (9).
- 9:     Calculating similarity between clients (10).
- 10:    Obtaining MAC (11).
- 11:    Calculating  $\hat{\mathbf{w}}_j^h$  and  $\hat{\mathbf{w}}_j^l$  (7) (14) (15).
- 12:    Aggregating global model parameters:  $\hat{\mathbf{w}}_j$  (13).
- 13:     $\hat{\Theta}^{t+1} = \{\hat{\mathbf{w}}_1, \dots, \hat{\mathbf{w}}_l\} \in \mathbb{R}^{l \times M}$ .
- 14: **return**  $\hat{\Theta}^T$

By calculating the dispersion of parameters from different clients, FedSA divides the parameters into high-dispersion and low-dispersion using a threshold. For the low-dispersion region, we calculate the client-dimension average of parameters, while for the high-dispersion region, we categorize these parameters based on Micro-Classes (MIC) and Macro-Classes (MAC) to extract exclusive information about clients. Figure 4 illustrates the detailed process of our proposed algorithm. Here, we consider the  $j$ -th layer parameters of the local model as an example, where the number of parameters is denoted by  $M$ ,  $\mathbf{w}_j \in \mathbb{R}^{K \times M}$ .

**Micro-Classes** In this section, We use the coefficient of variation (Brown 1998)  $cv_j$ , which owns prominent ability to discriminate dispersion statistically, to measure the discrepancies among the parameters from disparate clients.

$$\mu_j = \text{Mean}(\mathbf{w}_j) \in \mathbb{R}^{1 \times M}, \quad (2)$$

$$\mathbf{s}_j = \text{SD}(\mathbf{w}_j) \in \mathbb{R}^{K \times M}, \quad (3)$$

$$cv_j = \frac{\sqrt{\frac{1}{K} \mathbf{1}_{1 \times K} \mathbf{s}_j}}{|\mu_j|} \in \mathbb{R}^{1 \times M}. \quad (4)$$

$\text{SD}(\cdot)$  represents computing square deviation,  $\mathbf{r}_j^h, \mathbf{r}_j^l \in \mathbb{R}^{1 \times M}$  denotes the high-dispersion region and the low-dispersion region respectively. Based on hyperparameter  $cv_t$ , we determine  $\mathbf{r}_j^h$  and  $\mathbf{r}_j^l$  as follows:

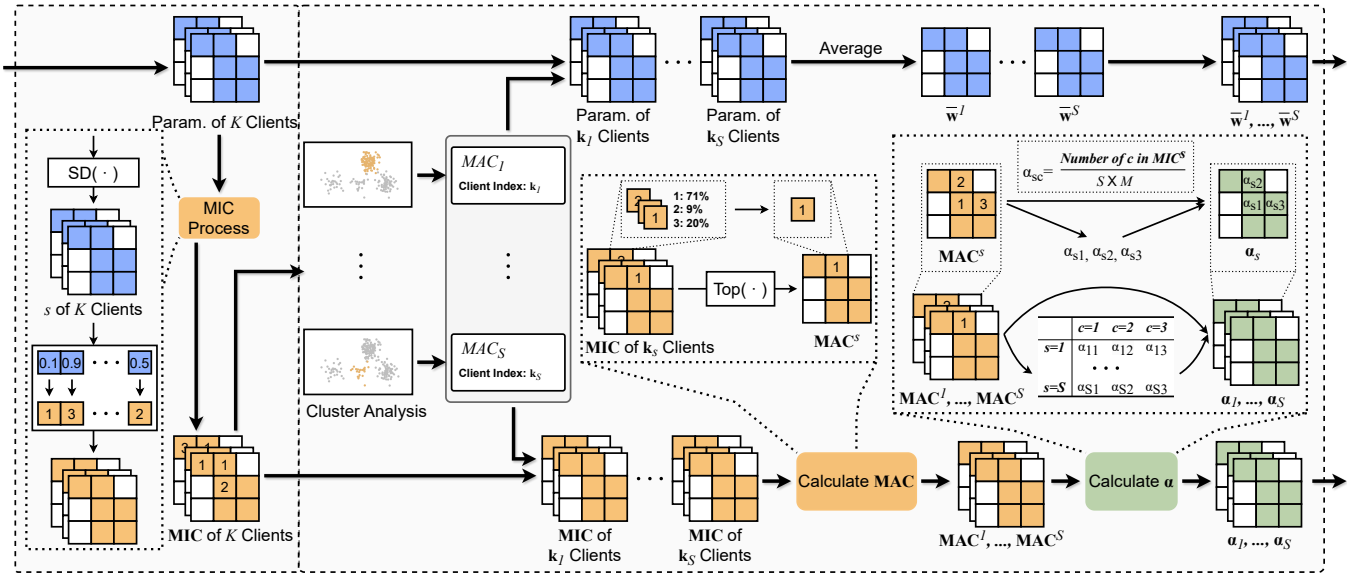


Figure 4: **The MIC-MAC Module architecture, including MIC (left) and MAC (right).** *Left:* We obtain mapping of Micro-Classes (MIC). The input, which consists of high-dispersion parameters, is processed by the MIC Process. *Right:* The input consists of the mapping of Micro-Classes (MIC) and clients' parameters. The output includes the weights of the global model's parameters ( $\alpha$ ) and the average parameter values for each Macro-Class.

$$\mathbf{r}_j^h = \mathbb{I}\left(\frac{\mathbf{cv}_j - \min(\mathbf{cv}_j)}{\max(\mathbf{cv}_j) - \min(\mathbf{cv}_j)} > cv_t\right), \quad (5)$$

$$\mathbf{r}_j^l = \mathbb{I}\left(\frac{\mathbf{cv}_j - \min(\mathbf{cv}_j)}{\max(\mathbf{cv}_j) - \min(\mathbf{cv}_j)} \leq cv_t\right). \quad (6)$$

In  $\mathbf{r}_j^l$ , the variation among the parameters of the clients' models is minimal. Consequently, we compute the average of these parameter values to determine the parameters of the global model.

$$\hat{\mathbf{w}}_j^l = \mathbf{r}_j^l \odot \mu_j \in \mathbb{R}^{1 \times M}. \quad (7)$$

For the parameters exhibiting significant differences among clients, denoted as  $\mathbf{r}_j^h$ , these are the areas of primary focus. The variation in these parameters reflects, to a certain extent, the distinct characteristics of the clients' models.

Due to the limitations of using a fixed threshold, which does not adequately account for the extent of parameter discrepancies in the high-dispersion region, we introduce Micro-Classes (MIC) and Macro-Classes (MAC) to describe the discrepancies. MIC and MAC, respectively, assess dispersion from the perspectives of local parameters and the global network.

MIC is formulated as follows:

$$\mathbf{I}_c = \mathbb{I}_c\left(\frac{c}{N} \geq s_j > \frac{c-1}{N}\right) \in \mathbb{R}^{K \times M}, \quad (8)$$

$$\mathbf{MIC}_j = \mathbf{1}_{K \times 1} \cdot \mathbf{r}_j^h \odot \sum_{c=1}^C \mathbf{I}_c = (\mathbf{mic}_1, \dots, \mathbf{mic}_k)^T \in \mathbb{R}^{K \times M}. \quad (9)$$

Let  $C$  denote the number of MIC parameter categories, where  $c = 1, \dots, C$ . The mapping of each parameter to category  $c$  is represented by  $\mathbf{I}_c$ , and  $\mathbb{I}_c$  indicates the positions assigned to category  $c$  that satisfy the given conditions. The vector **MIC** is composed of  $\mathbf{mic}_k$ , where  $\mathbf{mic}_k$  represents the distribution of category  $c$  within the  $k$ -th client.

**Macro-Classes** Intuitively, the training of a model is a holistic process, wherein local models exhibit synergistic effects. MIC only considers the differences between clients from a local parameter perspective. However, the differences in the global synergistic effects among local models are also crucial aspects that we need to focus on. This information can better reflect the characteristics of the models. Therefore, we propose Macro-Classes (MAC), which measure the similarity between clients based on the distribution of MIC across each model parameter. Using the MAC, we cluster and map the clients according to their similarity, resulting in the formation of MAC. These MACs effectively capture the exclusive information of each class of client.

Directly measuring the similarity between clients can be challenging. Therefore, we derive the similarity by calculating the degree of dissimilarity between clients:

$$\text{SIM}(a, b) = 1 - \frac{\text{Sum}(\mathbb{I}(\mathbf{mic}_a \neq \mathbf{mic}_b))}{\text{Count}(\mathbb{I}(\mathbf{r}_j^h = 1))}. \quad (10)$$

Here,  $\text{Sum}(\cdot)$  denotes the summation within a vector, and  $\text{Count}(\cdot)$  returns the number of non-zero elements.  $\text{SIM}(a, b)$  represents the similarity between client  $a$  and client  $b$ . We cluster the clients according to their similarity derived from Equation (10). The steps are as follows: **Step 1:** Merge the two clients with the highest similarity into a cluster. Calculate the average similarity of these two clients

Settings	Pathological heterogeneous setting			Practical heterogeneous setting			
Methods	CIFAR-10	CIFAR-100	Tiny-ImageNet	CIFAR-10	CIFAR-100	Tiny-ImageNet	CIFAR-100*
FedAvg	90.79±0.08	50.19±0.31	33.58±0.15	88.55±0.10	33.57±0.09	19.86±0.20	34.39±0.31
FedProx	90.75±0.08	50.08±0.30	32.98±0.08	88.94±0.08	34.10±0.39	19.64±0.22	34.39±0.30
MOON	90.65±0.16	50.42±0.11	33.82±0.07	88.78±0.25	33.91±0.15	19.72±0.15	34.64±0.04
FedGEN	90.52±0.10	50.38±0.66	32.77±0.42	88.84±0.23	34.16±0.17	19.42±0.50	35.00±0.11
FedNTD	90.22±0.12	50.71±0.49	34.05±0.47	88.60±0.10	33.90±0.32	19.57±0.09	34.79±0.45
Ditto	90.53±0.04	50.27±0.35	33.27±0.23	88.87±0.23	34.05±0.19	19.84±0.37	34.55±0.22
FedBABU	90.02±0.14	64.86±0.24	36.09±0.52	88.20±0.27	36.01±0.36	22.02±0.31	37.15±0.24
FedALA	90.47±0.28	50.10±0.28	33.26±0.25	88.81±0.15	33.75±0.04	19.62±0.22	34.80±0.07
FedSA(ours)	<b>91.36±0.23</b>	<b>69.72±0.25</b>	<b>39.27±0.39</b>	<b>90.41±0.17</b>	<b>39.09±0.19</b>	<b>25.41±0.37</b>	<b>39.12±0.04</b>

Table 1: **The test accuracy (%) in the pathological heterogeneous setting and practical heterogeneous setting.**

with all other clients to determine the similarity between the cluster and other clients. **Step 2:** If a client has the highest similarity with an existing cluster, merge it into that cluster; otherwise, merge the two clients with the highest similarity into a new cluster. **Step 3:** If the number of clusters reaches the upper limit  $S$ , there are two strategies for the remaining clients: if a client’s highest similarity with any cluster exceeds the threshold  $sim_t$ , merge the client into the cluster with the highest similarity; otherwise, mark the client as unclustered.

The clusters are denoted as  $\mathbf{K} = \mathbf{k}_1, \dots, \mathbf{k}_S$ , where  $\mathbf{k}_s \in \mathbb{R}^{1 \times K}$  records the indices of clients contained in the  $s$ -th cluster. The clusters encapsulate the aggregation tendencies of clients, which we refer to as MAC. Each  $MAC_s$  consists of three components: the indices of clients within the cluster  $\mathbf{k}_s$ ; the MIC aggregation entity  $\mathbf{MAC}_j^s$ ; and the parameter aggregation entity  $\bar{\mathbf{w}}_j^s$ .

$\mathbf{MAC}_j^s$  is derived from the MIC mapping of all clients within the cluster:

$$\mathbf{MAC}_j^s = \text{Top}(\text{Concat}(\mathbf{MIC}_{j, \mathbf{k}_s})) \in \mathbb{R}^{1 \times M}, \quad (11)$$

where  $\mathbf{MIC}_{j, \mathbf{k}_s}$  denotes the MIC vector for clients within the cluster.  $\text{Concat}(\cdot)$  performs concatenation of vectors, and  $\text{Top}(\cdot)$  returns the category with the highest frequency along the first dimension. The parameter aggregation entity  $\bar{\mathbf{w}}_j^s$  is the mean of the parameters from all clients within the cluster, and  $\mathbf{w}_{j, \mathbf{k}_s}$  represents the parameter vector of the clients within the cluster:

$$\bar{\mathbf{w}}_j^s = \text{Mean}(\mathbf{w}_{j, \mathbf{k}_s}) \in \mathbb{R}^{1 \times M}. \quad (12)$$

**Aggregation** Building on the methodologies discussed in Sections 3 and 3, we introduce a novel strategy for updating the global model, aimed at enhancing its quality. The parameters of the global model, denoted as  $\hat{\mathbf{w}}_j$ , are comprised of low dispersion parameters  $\hat{\mathbf{w}}_j^l$  and high dispersion parameters  $\hat{\mathbf{w}}_j^h$ . The procedure for computing these parameters is outlined as follows:

$$\hat{\mathbf{w}}_j = \hat{\mathbf{w}}_j^l + \hat{\mathbf{w}}_j^h, \quad (13)$$

where  $\hat{\mathbf{w}}_j^l$  is derived from Equation (7). We then iterate over the MAC and compute the aggregation weights  $\alpha_s$  for each

MAC, based on the distribution of the MIC aggregation entity.

$$\alpha_s = \sum_{c=1}^C \frac{\mathbb{I}(\mathbf{MAC}_j^s = c)}{S \times C} \mathbf{1}_{m \times 1} \cdot \mathbb{I}(\mathbf{MAC}_j^s = c) \in \mathbb{R}^{1 \times M} \quad (14)$$

We compute the dot product of the aggregation weights  $\alpha_s$  for each MAC with  $\bar{\mathbf{w}}_j^s$  to obtain the aggregated parameters for each MAC. Summing the aggregated parameters yields the high dispersion parameter aggregation result,  $\hat{\mathbf{w}}_j^h$ .

$$\hat{\mathbf{w}}_j^h = r_j^h \odot \sum_{s=1}^S \alpha_s \odot \bar{\mathbf{w}}_j^s \quad (15)$$

**Strategy** Deploying SA is straightforward, it only requires replacing the aggregation method in the FL system with SA. Therefore, by substituting the weighted average aggregation method in FedAVG with SA, we form FedSA. The complete steps of FedSA are detailed in Algorithm 1.

## 4 Experiments

### Experiment Setting

**Baselines** In this section, we select eight FL methods, encompassing both traditional federated learning (tFL) and personalized federated learning (pFL). TFL includes FedAVG (McMahan et al. 2017), FedProx (Li et al. 2020), MOON (Li, He, and Song 2021a), and FedNTD (Lee et al. 2022). Given that FedSA focuses on distinctive global models, we choose SOTA pFL methods that are capable of generating global models, including Ditto (Li et al. 2021), FedBABU (Oh, Kim, and Yun 2021), and FedALA (Zhang et al. 2023). Additionally, we illustrate the rationale of FedSA by utilizing the distribution of local models’ parameters, while also demonstrating the reason why other FL methods are unable to achieve good performance.

**Datasets** Our experiments are conducted on three widely used Computer Vision datasets, including CIFAR-10/100 and Tiny-ImageNet. The ratio of the train set to the test set is 0.75: 0.25. In this work, we simulate heterogeneous



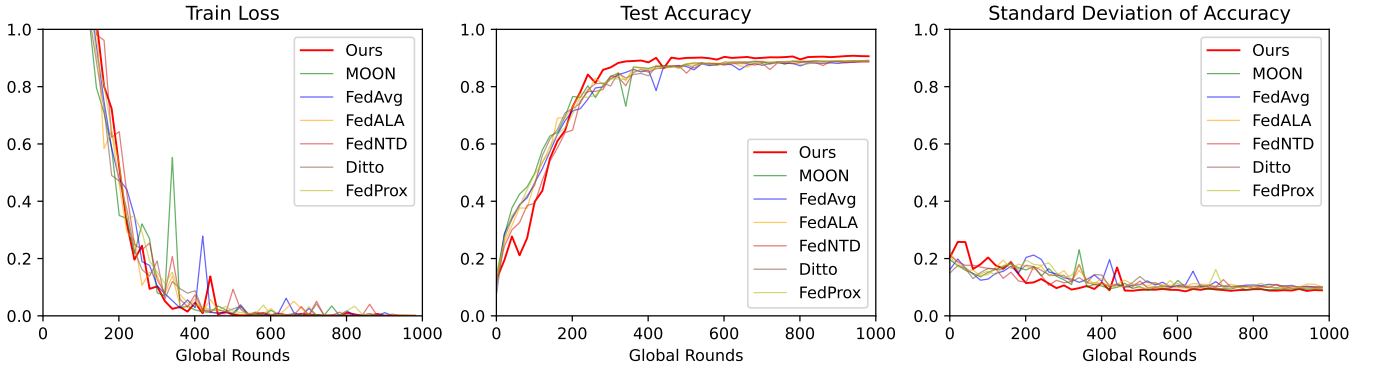


Figure 5: **The performance of FedSA(ours) and baselines on CIFAR-10.** The first figure presents the training loss of seven FL methods, while the second figure shows their test accuracy. Notably, the third figure depicts the standard deviation of clients’ test accuracy, where a lower value indicates less variation in accuracy among clients. Values are recorded every 20 rounds.

settings using pathological heterogeneity (McMahan et al. 2017; Shamsian et al. 2021; Zhang et al. 2023) and practical heterogeneity (Lin et al. 2020; Li, He, and Song 2021b). Regarding pathological heterogeneity, we allocate 2, 10, and 20 classes for CIFAR-10, CIFAR-100, and Tiny-ImageNet, respectively, to each client, while the classes for each client in the practical heterogeneity are controlled by the Dirichlet distribution  $\text{Dir}(\beta)$ . The smaller the  $\beta$ , the more severe the data heterogeneity. In this work, we set  $\beta=0.1$  for the experiments (Lin et al. 2020).

**Train Setting** To tackle the limitations of the simple CNN backbone in demonstrating SA’s performance, we employ ResNet-18 (He et al. 2016) as our backbone. Additionally, CIFAR-100\* represents that we carry out experiments with ResNet-34 (He et al. 2016) backbone on the CIFAR-100 dataset. On the server side, we set the global training rounds to 1000, the number of clients to 20, and the proportion of randomly selected clients per round  $\rho$  to 1.0. On the client side, we set the local training rounds per client to 1. Additionally, we compute the average testing accuracy of the global model over the last 10 rounds. We ran all tasks three times and reported the mean and standard deviation.

**Hyperparameter Setting** We set the threshold for distinguishing high-dispersion and low-dispersion regions,  $cv_t$ , to 0.2, and the minimum similarity between clients,  $sim_t$ , to 0.2. Specifically, we set the number of MIC  $C$  to 4, 5, and 8, and the number of MAC  $S$  to 4, 5, and 8 for CIFAR-10/100, and Tiny-ImageNet, respectively.

### Performance Comparison and Analysis

**Results** We evaluate the performance of FedSA against other baselines under different settings 4. Results in Table 1 illustrate that FedSA consistently outperforms the other eight FL algorithms in all scenarios. Specifically, in challenging CIFAR-100, our method offers an average improvement of about 5% and 3% respectively. When considering a pathological heterogeneous setting, where label classes from each dataset are fixed, notable improvements in accuracy are evident despite label skew. While the label skew is slight in practical heterogeneous settings, due to the Dirichlet-based

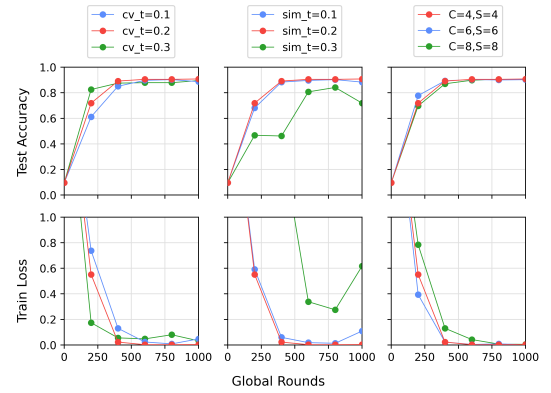


Figure 6: **The effect of each hyperparameter.** We demonstrate the effect of each hyperparameter on CIFAR-10, including  $cv_t$ ,  $sim_t$ ,  $C$ , and  $S$ . It is noticeable that various hyperparameters impact the performance of FedSA (ours) differently, especially  $sim_t$ . However, variations in  $C$  and  $S$  have only a slight influence on FedSA.

label distribution of datasets, FedSA outperforms others by about 3%. Meanwhile, FedBABU, a classical algorithm in pFL, trains professional local models with fine-tuning for each client. Our method not only surpasses FedBABU in every scenario but also has lower computation costs. Due to the poor generalization ability of the global model, FedAVG and FedProx perform poorly in two settings. As illustrated in Figure 5 under  $\text{Dir}(0.1)$ , we imagine the train loss, test accuracy and standard deviation of accuracy, which demonstrates the unsuspected stable performance of FedSA. In such experiments, FedSA exhibits comparable accuracy with the baselines.

**Effect of hyperparameter** We conducted experiments under different hyperparameter settings, the results are shown in Figure 6. Setting the threshold  $cv_t$  too high or too low can adversely affect our method’s performance, as it determines the number of parameters processed. As illustrated in Figure 6, optimal performance is achieved when  $cv_t$  is set

Methods	Scalability		
	$\rho = 1.0$ 50 clients	$\rho = 0.5$ 50 clients	$\rho = 0.5$ 100 clients
FedAvg	29.71 $\pm$ 0.11	29.72 $\pm$ 0.16	30.64 $\pm$ 0.19
FedProx	30.18 $\pm$ 0.51	30.14 $\pm$ 0.09	30.49 $\pm$ 0.39
MOON	29.91 $\pm$ 0.24	29.59 $\pm$ 0.18	30.65 $\pm$ 0.33
FedGen	29.74 $\pm$ 0.09	30.64 $\pm$ 0.21	30.36 $\pm$ 0.59
FedNTD	29.58 $\pm$ 0.19	29.90 $\pm$ 0.24	30.47 $\pm$ 0.19
Ditto	29.44 $\pm$ 0.21	30.24 $\pm$ 0.24	30.39 $\pm$ 0.13
FedBABU	30.08 $\pm$ 0.28	30.11 $\pm$ 0.45	30.79 $\pm$ 0.30
FedALA	29.60 $\pm$ 0.29	29.61 $\pm$ 0.27	30.44 $\pm$ 0.07
FedSA(ours)	<b>31.83<math>\pm</math>0.35</b>	<b>31.31<math>\pm</math>0.20</b>	<b>31.10<math>\pm</math>0.38</b>

Table 2: **The test accuracy (%) with various the number of clients and  $\rho$  on CIFAR-100**, which heterogeneity is Dir(0.1).

to 0.2. Similarly, setting  $sim_t$  too high (e.g.,  $sim_t = 0.3$ ) reduces the number of training clients, leading to diminished model performance. Smaller values of  $C$  and  $S$  lower computational costs and accelerate the convergence of our method. Therefore, we favor smaller  $C$  and  $S$ , provided test accuracy is maintained.

**Heterogeneity** To study the effectiveness of FedSA in the settings with different degrees of heterogeneity, we vary the  $\beta$  in Dir( $\beta$ ) on CIFAR-100. The smaller  $\beta$  is, the more heterogeneity the setting is. In Table 3, most FL methods exhibit improved performance in more heterogeneous settings. Notably, FedSA consistently outperforms the other seven FL methods across all settings. With Dir(0.01), our method achieves the highest test accuracy at 74.39%.

**Scalability** To demonstrate the scalability of FedSA, we conduct experiments with 50 and 100 clients, using  $\rho$  values of 0.5 and 1.0 in the default heterogeneous setting. As shown in Table 2, most FL methods experience significant degradation when the number of clients decreases to 50, while FedSA remains relatively stable. Given the constant data volume of CIFAR-100, each local model captures specific information. Our method effectively captures the main information from most local models, showing minimal sensitivity to the number of clients. Additionally, increasing  $\rho$  to 1.0, which means more data is processed by FedSA in each round, leads to performance improvements for FedSA. In contrast, the performance of other methods remains nearly unchanged.

## Model Analysis

Aiming to illustrate the rationale behind FedSA, we visualize the distribution of parameters in local models and global models from different methods. From Figure 2, it is evident that the distribution of most parameters across different client models is skewed, which supports *parameter skew*. This skewness contributes to the weak generalization ability of the FL algorithm. For example, FedAVG directly averages these parameters, but according to the Law of Large Num-

Methods	Heterogeneity		
	Dir(0.01)	Dir(0.5)	Dir(1)
FedAvg	48.42 $\pm$ 0.48	36.04 $\pm$ 0.18	37.46 $\pm$ 0.14
FedProx	48.62 $\pm$ 0.66	36.39 $\pm$ 0.19	37.47 $\pm$ 0.12
MOON	47.76 $\pm$ 0.41	36.07 $\pm$ 0.18	37.21 $\pm$ 0.11
FedGen	51.07 $\pm$ 0.81	36.18 $\pm$ 0.28	37.61 $\pm$ 0.22
FedNTD	48.48 $\pm$ 0.71	36.38 $\pm$ 0.35	37.63 $\pm$ 0.10
Ditto	48.57 $\pm$ 0.71	36.18 $\pm$ 0.26	37.55 $\pm$ 0.22
FedBABU	71.67 $\pm$ 0.16	35.44 $\pm$ 0.12	36.58 $\pm$ 0.42
FedALA	48.34 $\pm$ 0.30	36.32 $\pm$ 0.15	37.37 $\pm$ 0.03
FedSA(ours)	<b>74.39<math>\pm</math>0.66</b>	<b>38.13<math>\pm</math>0.41</b>	<b>39.41<math>\pm</math>0.10</b>

Table 3: **The test accuracy (%) with different heterogeneous settings on CIFAR-100**, which the number of clients is 20, and  $\rho$  is 1.0.

bers, the mean of a skewed distribution can be biased by extreme values, resulting in overestimation or underestimation, which can hinder the global model’s ability to generalize.

As shown in Figure 2, the parameters of the FedAVG global model deviate from the main tendency. However, FedSA accounts for *parameter skew*. By maintaining the computation and communication costs, it adjusts the global model’s parameter values to better align with the overall trend. Therefore, our method enables the global model to capture the characteristics of most local models, enhancing its generalization ability. This explains the significant advantage of FedSA in updating the global model’s parameters.

## 5 Conclusion and Discussions

### Conclusion

Federated learning has become a promising method to resolve the pain of silos in many domains such as medical imaging and micro-model deployment. The heterogeneity of data is the key challenge for the performance of federated learning. We propose FedSA, a novel and conducive approach for federated learning, to enhance the performance of federated deep learning models on non-IID datasets. FedSA introduces a conception, *parameter skew*, and tackles the implication of it. Our extensive experiments show that FedSA achieves great improvements over state-of-the-art approaches in various scenarios. Moreover, we analyze the rationale behind our method and demonstrate why other federated learning methods fail to achieve good performance.

### Discussions

**Limitation** For lack of computation resources and a tight schedule, at this time we could not further compare more advanced FL methods and fully investigate the potential of FedSA on larger models.

**Future Work** FedSA is designed based on the discrete distance between clients, and we will further explore the performance of other methods for measuring discrepancy. Moreover, We will investigate the impact of parameter skew

on the FL system and observe its performance under different settings.

## 6 Acknowledgements

This research was supported by the National Natural Science Foundation of China (12371272), and the Basic Research Project of Shanghai Science and Technology Commission (22JC1400800).

## References

- Brown, C. E. 1998. Coefficient of variation. In *Applied multivariate statistics in geohydrology and related sciences*, 155–157. Springer.
- Chen, Z.; Liu, S.; Wang, H.; Yang, H. H.; Quek, T. Q.; and Liu, Z. 2022. Towards federated long-tailed learning. *arXiv preprint arXiv:2206.14988*.
- Chrabaszcz, P.; Loshchilov, I.; and Hutter, F. 2017. A down-sampled variant of imagenet as an alternative to the cifar datasets. *arXiv preprint arXiv:1707.08819*.
- He, K.; Zhang, X.; Ren, S.; and Sun, J. 2016. Deep residual learning for image recognition. In *Proceedings of the IEEE conference on computer vision and pattern recognition*, 770–778.
- Hsu, P.-L.; and Robbins, H. 1947. Complete convergence and the law of large numbers. *Proceedings of the national academy of sciences*, 33(2): 25–31.
- Kairouz, P.; McMahan, H. B.; Avent, B.; Bellet, A.; Bennis, M.; Bhagoji, A. N.; Bonawitz, K.; Charles, Z.; Cormode, G.; Cummings, R.; et al. 2021. Advances and open problems in federated learning. *Foundations and trends® in machine learning*, 14(1–2): 1–210.
- Karimireddy, S. P.; Kale, S.; Mohri, M.; Reddi, S.; Stich, S.; and Suresh, A. T. 2020. Scaffold: Stochastic controlled averaging for federated learning. In *International conference on machine learning*, 5132–5143. PMLR.
- Krizhevsky, A.; Hinton, G.; et al. 2009. Learning multiple layers of features from tiny images.
- Lee, G.; Jeong, M.; Shin, Y.; Bae, S.; and Yun, S.-Y. 2022. Preservation of the global knowledge by not-true distillation in federated learning. *Advances in Neural Information Processing Systems*, 35: 38461–38474.
- Li, Q.; He, B.; and Song, D. 2021a. Model-contrastive federated learning. In *Proceedings of the IEEE/CVF conference on computer vision and pattern recognition*, 10713–10722.
- Li, Q.; He, B.; and Song, D. 2021b. Model-contrastive federated learning. In *Proceedings of the IEEE/CVF conference on computer vision and pattern recognition*, 10713–10722.
- Li, T.; Hu, S.; Beirami, A.; and Smith, V. 2021. Ditto: Fair and robust federated learning through personalization. In *International conference on machine learning*, 6357–6368. PMLR.
- Li, T.; Sahu, A. K.; Zaheer, M.; Sanjabi, M.; Talwalkar, A.; and Smith, V. 2020. Federated optimization in heterogeneous networks. *Proceedings of Machine learning and systems*, 2: 429–450.
- Lin, T.; Kong, L.; Stich, S. U.; and Jaggi, M. 2020. Ensemble distillation for robust model fusion in federated learning. *Advances in neural information processing systems*, 33: 2351–2363.
- Liu, Y.; Huang, A.; Luo, Y.; Huang, H.; Liu, Y.; Chen, Y.; Feng, L.; Chen, T.; Yu, H.; and Yang, Q. 2020. Fedvision: An online visual object detection platform powered by federated learning. In *Proceedings of the AAAI conference on artificial intelligence*, volume 34, 13172–13179.
- McMahan, B.; Moore, E.; Ramage, D.; Hampson, S.; and y Arcas, B. A. 2017. Communication-efficient learning of deep networks from decentralized data. In *Artificial intelligence and statistics*, 1273–1282. PMLR.
- Oh, J.; Kim, S.; and Yun, S.-Y. 2021. Fedbabu: Towards enhanced representation for federated image classification. *arXiv preprint arXiv:2106.06042*.
- Shamsian, A.; Navon, A.; Fetaya, E.; and Chechik, G. 2021. Personalized federated learning using hypernetworks. In *International Conference on Machine Learning*, 9489–9502. PMLR.
- Shang, X.; Lu, Y.; Huang, G.; and Wang, H. 2022. Federated learning on heterogeneous and long-tailed data via classifier re-training with federated features. *arXiv preprint arXiv:2204.13399*.
- Shokri, R.; and Shmatikov, V. 2015. Privacy-preserving deep learning. In *Proceedings of the 22nd ACM SIGSAC conference on computer and communications security*, 1310–1321.
- T Dinh, C.; Tran, N.; and Nguyen, J. 2020. Personalized federated learning with moreau envelopes. *Advances in neural information processing systems*, 33: 21394–21405.
- Van der Maaten, L.; and Hinton, G. 2008. Visualizing data using t-SNE. *Journal of machine learning research*, 9(11).
- Venkateswaran, P.; Isahagian, V.; Muthusamy, V.; and Venkatasubramanian, N. 2023. Fedgen: Generalizable federated learning for sequential data. In *2023 IEEE 16th International Conference on Cloud Computing (CLOUD)*, 308–318. IEEE.
- Wang, H.; Kaplan, Z.; Niu, D.; and Li, B. 2020a. Optimizing federated learning on non-iid data with reinforcement learning. In *IEEE INFOCOM 2020-IEEE conference on computer communications*, 1698–1707. IEEE.
- Wang, H.; Yurochkin, M.; Sun, Y.; Papailiopoulos, D.; and Khazaeni, Y. 2020b. Federated learning with matched averaging. *arXiv preprint arXiv:2002.06440*.
- Wu, Q.; Chen, X.; Zhou, Z.; and Zhang, J. 2020. Fed-home: Cloud-edge based personalized federated learning for in-home health monitoring. *IEEE Transactions on Mobile Computing*, 21(8): 2818–2832.
- Yang, Q.; Liu, Y.; Chen, T.; and Tong, Y. 2019. Federated machine learning: Concept and applications. *ACM Transactions on Intelligent Systems and Technology (TIST)*, 10(2): 1–19.
- Yang, Q.; Zhang, J.; Hao, W.; Spell, G. P.; and Carin, L. 2021. Flop: Federated learning on medical datasets using partial networks. In *Proceedings of the 27th ACM SIGKDD*



Zhang, J.; Hua, Y.; Wang, H.; Song, T.; Xue, Z.; Ma, R.; and Guan, H. 2023. Fedala: Adaptive local aggregation for personalized federated learning. In *Proceedings of the AAAI Conference on Artificial Intelligence*, volume 37, 11237–11244.

## A Additional Results

**Communication and Computation Cost** We record the total time cost for each method until convergence, as shown in Table 4. FedSA costs 0.248 min (similar to FedAVG) in each iteration. In other words, our method only costs an additional 0.002 min for great accuracy improvement. Moreover, we show the communication cost for one client in one iteration in Table 4. The communication overhead for most methods is the same as FedAVG, which uploads and downloads only one model.

**Scalability** Table 5 shows the result of CIFAR-10 with the same scalability setting.

	Computation		Communication
	Total time	Time/iter.	Param./iter.
FedAvg	208 min	0.246 min	$2 * \Sigma$
FedProx	245 min	0.286 min	$2 * \Sigma$
MOON	402 min	0.401 min	$2 * \Sigma$
FedGen	307 min	0.508 min	$2 * \Sigma$
FedNTD	465 min	0.302 min	$2 * \Sigma$
Ditto	265 min	0.523 min	$2 * \Sigma$
FedBABU	246 min	0.245 min	$2 * \alpha_f * \Sigma$
FedALA	210 min	0.249 min	$2 * \Sigma$
FedSA	225 min	0.248 min	$2 * \Sigma$

Table 4: **The computation cost on CIFAR-10 and the communication cost (transmitted parameters per iteration).**  $\Sigma$  is the parameter amount in the backbone.  $\alpha_f$  ( $\alpha_f < 1$ ) is the ratio of the parameters of the feature extractor in the backbone.

## B Hyperparameter Settings

The hyperparameter settings for all FL methods in this work are as follows:

- For FedProx, the proximal term adjusts the distance between the local model and global model, we set the coefficient of proximal term  $\mu$  to 0.001.
- For MOON, the temperature parameter controls the similarity between the local model and global model when calculating the contrast loss, we set the temperature parameter  $\tau$  to 1.0.
- For FedGen, FedGen generates a generator and broadcasts it to all clients, we set the learning rate of the generator to 0.005, the hidden dim of the generator to 512, and the localize feature extractor to False. To diversify

Methods	Scalability		
	$\rho = 1.0$ 50 clients	$\rho = 0.5$ 50 clients    100 clients	
FedAvg	84.80±0.24	84.91±0.31	88.09±0.19
FedProx	84.86±0.27	84.24±0.66	88.45±0.13
MOON	84.64±0.18	84.47±0.59	87.72±0.18
FedGen	84.73±0.31	<b>85.65±0.30</b>	87.67±0.38
FedNTD	83.40±0.10	83.95±0.09	86.33±0.27
Ditto	84.34±0.22	84.91±0.54	88.02±0.20
FedBABU	84.06±0.10	84.57±0.19	87.02±0.19
FedALA	84.18±0.26	84.76±0.21	87.81±0.14
FedSA	<b>87.24±0.14</b>	84.53±0.13	<b>88.63±0.22</b>

Table 5: **The test accuracy (%) with various the number of clients and  $\rho$  on CIFAR-10**, which heterogeneity is Dir(0.1).

the output of the generator, the authors introduce a noise vector to the generator, we set the noise dim to 512.

- For Ditto, the client adjusts the preferences of the personalized model in the global model and the local model through the hyperparameter  $\lambda$ , we set the hyperparameter  $\lambda$  to 0.001.
- For FedBABU, FedBABU fine-tunes the classifier of the global model for clients, we set the fine-tuning epochs to 10.
- For FedALA, we set the parameter for random select parameters rate to 0.8, the applying ALA on higher layers number to 1.
- For FedSA, we set the parameter for the threshold of coefficient of variation to 0.2, and the threshold of similarity to 0.2, specially, we set the number of MIC and MAC to 4 and 4, 5 and 5, 8 and 8 for CIFAR-10/CIFAR-100/Tiny-ImageNet.

## C Data Distribution Visualization

Figure 7 shows the distribution of labels under the IID setting, pathological setting, and practical setting. Figure 8 further shows the distribution of labels under different practical settings.

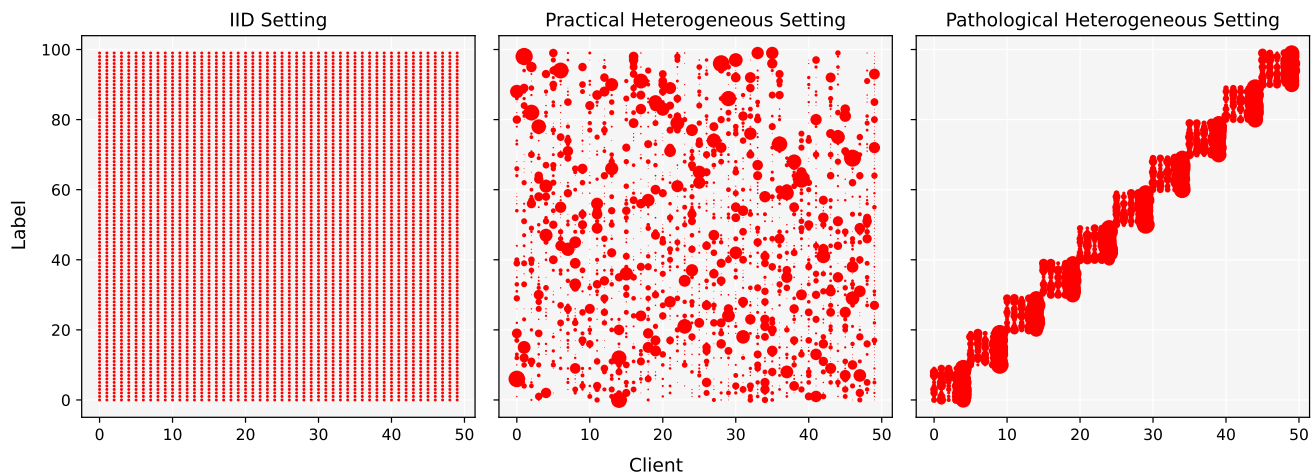


Figure 7: **The distribution of CIFAR-100 data under the IID setting, pathological setting, and practical setting**, in which the number of clients is 50. The size of the circle represents the number of samples.

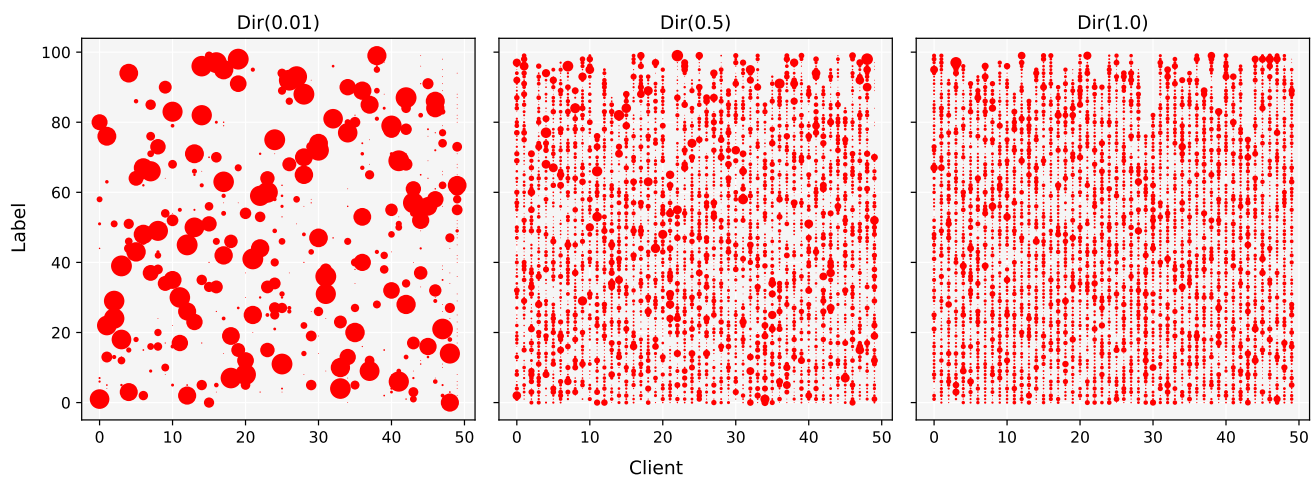


Figure 8: **The distribution of CIFAR-100 data under the Dir(0.01), Dir(0.5), Dir(1.0) heterogeneous setting**, which the number of clients is 50. The size of the circle represents the number of samples.